PALEOCEANOGRAPHY, VOL. 19, PA4029, doi:10.1029/2003PA000892, 2004

Correction published 30 March 2005

Forcing of tropical Atlantic sea surface temperatures during the mid-Pleistocene transition

Enno Schefuß,[1] Jaap S. Sinninghe Damsté, and J. H. Fred Jansen
Royal Netherlands Institute for Sea Research, Den Burg, Netherlands

Received 12 February 2003; revised 28 September 2004; accepted 25 October 2004; published 28 December 2004.

[1] We compare a new mid-Pleistocene sea surface temperature (SST) record from the eastern tropical Atlantic to changes in continental ice volume, orbital insolation, Atlantic deepwater ventilation, and Southern Ocean front positions to resolve forcing mechanisms of tropical Atlantic SST during the mid-Pleistocene transition (MPT). At the onset of the MPT, a strong tropical cooling occurred. The change from a obliquity- to a eccentricity-dominated cyclicity in the tropical SST took place at about 650 kyr BP. In orbital cycles, tropical SST changes significantly preceded continental ice-volume changes but were in phase with movements of Southern Ocean fronts. After the onset of large-amplitude 100-kyr variations, additional late glacial warming in the eastern tropical Atlantic was caused by enhanced return flow of warm waters from the western Atlantic driven by strong trade winds. Pronounced 80-kyr variations in tropical SST occurred during the MPT, in phase with and likely directly forced by transitional continental ice-volume variations. During the MPT, a prominent anomalous long-term tropical warming occurred, likely generated by extremely northward displaced Southern Ocean fronts. While the overall pattern of global climate variability during the MPT was determined by changes in mean state and frequency of continental ice volume variations, tropical Atlantic SST variations were primarily driven by early changes in Subantarctic sea-ice extent and coupled Southern Ocean frontal positions. *INDEX TERMS:* 1620 Global Change: Climate dynamics (3309); 3344 Meteorology and Atmospheric Dynamics: Paleoclimatology; 4267 Oceanography: General: Paleoceanography; 9325 Information Related to Geographic Region: Atlantic Ocean; *KEYWORDS:* sea surface temperatures, mid-Pleistocene transition, tropical Atlantic

Citation: Schefuß, E., J. S. Sinninghe Damsté, and J. H. F. Jansen (2004), Forcing of tropical Atlantic sea surface temperatures during the mid-Pleistocene transition, *Paleoceanography*, *19*, PA4029, doi:10.1029/2003PA000892.

1. Introduction

[2] The mid-Pleistocene transition (MPT) led to the development of the late Pleistocene ice ages with increased mean continental ice volume changing in a sawtooth-like pattern in near-100-kyr cycles [*Mudelsee and Schulz*, 1997; *Prell*, 1982]. Records related to ice volume are dominated by 41-kyr variations before the 100-kyr rhythm became dominant [*Pisias and Moore*, 1981; *Ruddiman et al.*, 1989; *Shackleton and Opdyke*, 1976]. The increase in mean continental ice mass has been reported to be an abrupt event at 900 kyr BP [*Maasch*, 1988; *Prell*, 1982], whereas later studies favor an increase lasting from about 920 to 900 kyr BP [*Berger and Jansen*, 1994] or from 942 to 902 kyr BP [*Mudelsee and Schulz*, 1997], i.e., occurring essentially during marine isotope stage (MIS) 24. The transition from a predominant 41 kyr to a predominant 100-kyr cycle has been considered to have been both gradual as well as abrupt. A gradual increase was favored by *Ruddiman et al.* [1989] and *Berger and Jansen* [1994]. They placed it between 900 and 400 kyr BP, with the strongest change occurring between 700 and 600 kyr BP. *Park and Maasch* [1993] concluded that the transition occurred gradually between 1000 and 500 kyr BP. *Bolton et al.* [1995] inferred a stepwise transition with strongest changes around 750 kyr BP. An abrupt increase in power of the 100-kyr cycle, however, was placed at 900 kyr BP [*Pisias and Moore*, 1981], at 700 kyr BP [*Lau and Weng*, 1995], and at 641 kyr BP [*Mudelsee and Schulz*, 1997]. In either way, it is generally agreed that the increase in mean continental ice mass significantly preceded the increase in spectral power of the 100-kyr cycle [*Mudelsee and Schulz*, 1997].

[3] To examine how the changes in mean state and frequency of the continental ice-volume changes were related to the low-latitude climate, we compare a new mid-Pleistocene SST record from the tropical Atlantic with the history of continental ice volume, orbital insolation changes, variations in Atlantic deepwater ventilation, and past frontal movements in the Southern Ocean. The establishment of a tropical SST record extending far beyond the 100-kyr dominance of high-latitude climate changes allows resolving the (changing) importance of the various potential climatic forcing mechanisms and their phase relations during the MPT.

1.1. Hydrography of the Angola Basin

[4] The sea surface temperature (SST) record for the MPT is derived from core ODP 1077 (10°26.2′E, 5°10.8′S, 2382 m water depth), located in the tropical Atlantic Angola Basin about 275 km off the mouth of the Congo River

[1]Now at Department of Marine Chemistry and Geochemistry, Woods Hole Oceanographic Institution, Woods Hole, Massachusetts, USA.

Copyright 2004 by the American Geophysical Union.
0883-8305/04/2003PA000892$12.00

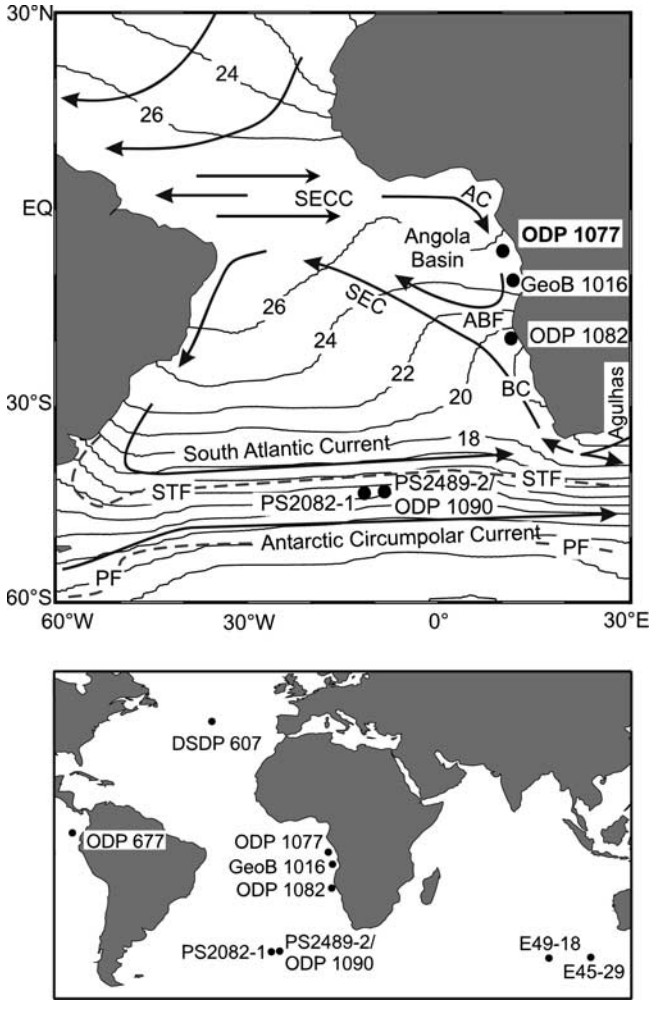

Figure 1. Map showing the locations of ODP Site 1077 and other cores discussed as well as the surface and shallow subsurface circulation in the South Atlantic Ocean. AC, Angola Current; BC, Benguela Current; SEC, South Equatorial Current; SECC, South Equatorial Countercurrent; ABF, Angola-Benguela Front; STF, subtropical front; PF, polar front. The thin lines are isotherms of modern annual mean SST [*Levitus and Boyer*, 1994]. The overview map shows the locations of all discussed sediment cores.

[*Wefer et al.*, 1998]. The modern surface and shallow subsurface hydrography in the Angola Basin is a cyclonic gyre circulation connected to the tropical Atlantic warm pool (Figure 1, e.g., [*Peterson and Stramma*, 1991]). Warm tropical waters flow eastward in the South Equatorial Counter Current (SECC) and feed the Angola Current (AC) flowing southward along the Central African margin. Between 14°S to 17°S its warm waters converge with the northward flowing cold Benguela Current (BC). A frontal zone, the Angola-Benguela Front (ABF), is established and extends up to 1000 km offshore [*Meeuwis and Lutjeharms*, 1990]. The joined waters of the Angola and Benguela Current are deflected to the northwest and form the South Equatorial Current (SEC) flowing northwestward to the equator. The ABF is the northern boundary of the zonally directed southeasterly (SE) trade winds and forms an effective barrier for surface-ocean mixing [*Meeuwis and Lutjeharms*, 1990]. South of the ABF, the BC transports relatively cold waters derived from the South Atlantic Current and relatively warm Indian Ocean waters derived via the Agulhas leakage northward [*Lutjeharms and van Ballegooyen*, 1988]. The BC is driven predominantly by the SE trade winds, which induce upwelling of cold South Atlantic Central Water off the coast of South Africa and Namibia [*Shannon*, 1985]. Coastal upwelling north of the ABF is restricted to small-scale upwelling cells near the Congo River mouth, far away from ODP Site 1077.

[5] The low-salinity plume of the Congo River can be detected as far as 800 km offshore [*van Bennekom and Berger*, 1984] and overprints the surface water circulation of the Angola Basin at 5°S. The seasonal variation in river discharge is related to monsoonal circulation and precipitation changes [*Eisma and van Bennekom*, 1978; *van Bennekom and Berger*, 1984]. During austral summer (December to February) the Intertropical Convergence Zone (ITCZ) is in its southernmost position, causing maximum monsoonal conditions with high precipitation in equatorial and southern Africa [*Hsü and Wallace*, 1976]. The maximum extension of the Congo River plume occurs in February–March, later than the maximum discharge in December [*van Bennekom and Berger*, 1984] and is associated with the highest annual SSTs in the Angola Basin [*Katz and Garzoli*, 1982]. During austral winter (June to August), the ITCZ is furthest north and strong SE trade winds blow over the Angola Basin. Offshore oceanic upwelling by surface divergence [*Philander and Pacanowski*, 1986] causes annual minimum SSTs during austral winter [*Katz and Garzoli*, 1982].

1.2. Late Quaternary Tropical Atlantic Paleoceanography

[6] Alkenone-derived SST estimates are generally assumed to reflect annual mean mixed layer temperatures [*Müller et al.*, 1998]. For the Angola Basin this is corroborated by core top data from sediments off the Congo and Angola [*Schneider et al.*, 1995], which are in excellent agreement with modern annual mean SST values [*Levitus and Boyer*, 1994]. A comparison of two late Quaternary sedimentary alkenone-SST records, from the lower Congo fan and offshore the Angolan coast, showed that the Congo freshwater outflow had only a minor effect on SST variations [*Schneider et al.*, 1995]. The two SST records covary strongly and exhibit the same temperature range [*Schneider et al.*, 1995]. They also closely follow the SST development in the eastern equatorial Atlantic [*Mix et al.*, 1986]. The late Quaternary SST records from the Angola Basin are dominated by periods of 100 and 23 kyr, while variance in the 41-kyr cycle is absent [*Schneider et al.*, 1999, 1995, 1996]. The precessional SST variations in the eastern equatorial Atlantic were inferred to be mainly a wind-forced phenomenon [*Schneider et al.*, 1996]. Every 23 kyr, when boreal summer insolation reaches a maximum, the SE trade winds over the Angola Basin are deflected northward and blow in a more meridional direction, suppressing the oceanic upwelling intensity [*McIntyre et al.*, 1989]. Oceanic diver-

gence responds almost immediately to changes in direction and strength of the trade winds [*Imbrie et al.*, 1989]. The late Quaternary precessional SST changes in the Angola Basin thus only slightly lag the Southern Hemisphere SST changes, but significantly lead over high-latitude Northern Hemisphere SST and continental ice-volume changes [*McIntyre et al.*, 1989; *Schneider et al.*, 1996]. Low-latitude insolation therefore is the dominant forcing for the 23-kyr cyclic SST variations.

[7] The late Quaternary SST variations in the eccentricity band, however, have mainly been explained by influences of high-latitude processes. When, during times of enlarged continental ice volume and sea-ice extent, Subantarctic oceanic fronts were shifted northward, the Southern Hemisphere thermal gradient was increased [*McIntyre et al.*, 1989]. Owing to the compressed atmospheric circulation the zonal velocity of the SE trades was amplified [*de Menocal and Rind*, 1993; *Manabe and Broccoli*, 1985], increasing upwelling in the Angola Basin due to oceanic divergence [*Jansen et al.*, 1996; *Schneider et al.*, 1996]. Simultaneously, the advection of heat from southern high latitudes decreased. During glaciations, the subtropical front was displaced to the north, reducing or perhaps even pinching off the inflow of warm Indian Ocean waters into the South Atlantic [*Rau et al.*, 2002]. These processes, wind-driven upwelling and cold water advection, thus both depend on oceanic front positions in the Southern Ocean. The late Quaternary SST changes in the eccentricity band have been found to significantly lead over continental ice volume changes [*Schneider et al.*, 1999, 1996]. It was suggested that the early tropical warming was caused by (1) heat storage in the tropical oceans due to a reduced thermohaline circulation (THC), or (2) enhanced flow of warm tropical waters into the Angola Basin during peak glacial times [*Schneider et al.*, 1996]. Reduced THC is expected to decrease the northward heat export from the tropical South Atlantic and to warm tropical Atlantic surface waters [*Crowley*, 1992]. This process has been inferred for short-term climate variations in the late Pleistocene [*Kim et al.*, 2003; *Rühlemann et al.*, 2004, 1999]. The second process is presently observed during austral winter, when strong SE trade winds enhance water and heat transport with the SEC into the western Atlantic. Part of the SEC is deflected backward at the Brazilian coast and flows as warm SECC toward the eastern tropical Atlantic [*Philander and Pacanowski*, 1986]. It has been proposed that this return flow of warm waters was more important during times of strongest SE trade winds, such as the Last Glacial Maximum [*Schneider et al.*, 1996] and the Younger Dryas [*Kim et al.*, 2003]. The sole occurrence of the 100- and 23-kyr cycles, and absence of the 41-kyr period, in late Quaternary SST records from the tropical Atlantic, combined with the early warming, has, however, also led to the suggestion that tropical SST variations may be a direct response to low-latitude insolation forcing and not being related to high-latitude climatic changes [*Schneider et al.*, 1999].

2. Material and Methods

[8] The samples for this study were obtained from the ODP Site 1077 (Figure 1). The uppermost sample investigated is 175-1077-B-8-H-1-17 cm, 62.77 meters below seafloor (mbsf) and the lowermost sample is 175-1077-B-17-H-6-33 cm, at 155.93 mbsf. The stratigraphy of ODP Site 1077 is based on correlation of its oxygen-isotope record of planktonic foraminifera (only *Globigerinoides ruber* (pink) was consistently present) to the benthic oxygen-isotope record of the eastern Pacific ODP Site 677 [*Dupont et al.*, 2001; *Shackleton et al.*, 1990]. The sedimentation rates in the investigated depth interval are high, around 12 cm/kyr, and quite constant; likely a result of a sustained supply of fine, suspended material by the river and high productive overlying waters [*Berger et al.*, 1998; *Dupont et al.*, 2001; *Jansen et al.*, 1984]. The ages for all 214 samples were determined by linear interpolation between the tie points using the revised composite-depth scale [*Jansen and Dupont*, 2001]. On the basis of this stratigraphy, the investigated samples cover the time interval from MIS 12 to 37, i.e., from 457 to 1250 kyr BP. The average time resolution of the SST record is 3.9 kyr. The age model of ODP 1077 is thus sufficiently accurate to investigate phase relations in the 100- and 41-kyr cycles, but not to address the phasing in the precessional cycle [*Dupont et al.*, 2001].

[9] SST estimates were determined with the alkenone-unsaturation method [*Brassell et al.*, 1986]. About 5 to 10 g of freeze-dried and ground sediments were ultrasonically extracted using 40 mL of methanol (MeOH), 40 mL of dichloromethane (DCM):MeOH (1:1, v/v), and 40 mL of DCM, each for 5 min. For each sample, extracts were combined and rotary-evaporated to near-dryness. Salts were removed by washing the extracts with double-distilled H_2O and re-extraction of the lipids with DCM. The desalted lipid extracts were again rotary-evaporated and methylated with diazomethane after drying over anhydrous Na_2SO_4. Before silylation with bis(trimethyl-silyl)trifluoro-acetamide in pyridine (1 hr at 60°C), very polar compounds were removed on a silica-gel column eluted with ethyl acetate. For gas chromatographic analyses extracts were concentrated to about 1 mg/ml. Capillary gas chromatography was performed using a Hewlett Packard 5890 series II gas chromatograph equipped with an on-column injector and fitted with a fused-silica capillary column (25 m × 0.32 mm) coated with CP Sil 5. The oven was programmed from 70°C to 130°C at 20°C/min, followed by a heating of 4°C/min to 320°C (10 min holding time). Components were detected using a flame ionization detector (FID). Compound identification and purity was checked on randomly selected samples by GC-mass spectrometry (GC-MS), performed using the same type of gas chromatograph and conditions described above using a VG Autospec Ultima mass spectrometer. Compound identifications were based on comparison with published mass spectra [*de Leeuw et al.*, 1980].

[10] For SST estimation, we used the simplified unsaturation index of the C_{37} alkenones ($U^{K'}_{37}$) [*Prahl and Wakeham*, 1987], calculated from the peak areas of the diunsaturated and triunsaturated C_{37} alkenones in FID chromatograms. The conversion of $U^{K'}_{37}$ values to SST estimates was done using the global calibration by *Müller et al.* [1998]: SST (°C) = $(U^{K'}_{37} - 0.044)/0.033$. The standard error of this relationship is ±1.0°C. The standard deviation (σ) based on

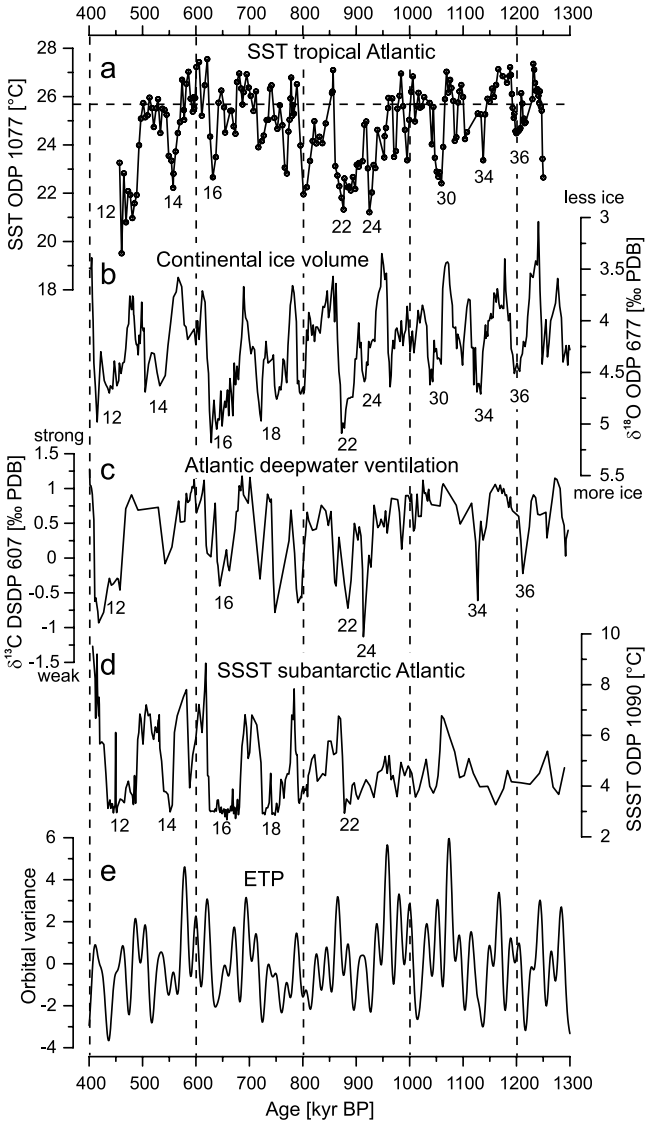

Figure 2. The investigated time series for the mid-Pleistocene transition: (a) ODP Site 1077 tropical SST, (b) ODP Site 677 benthic $\delta^{18}O$ reflecting continental ice-volume variations (note axis orientation) [*Shackleton et al.*, 1990], (c) DSDP Site 607 benthic $\delta^{13}C$ reflecting the strength of Atlantic deepwater ventilation [*Raymo et al.*, 1997; *Ruddiman et al.*, 1989], (d) Subantarctic summer sea-surface temperatures from ODP Site 1090 [*Becquey and Gersonde*, 2002], and (e) the calculated ETP record of orbital variance [*Berger and Loutre*, 1991; *Imbrie et al.*, 1984]. The horizontal broken line in Figure 2a is the modern annual mean at the location of ODP 1077 [*Levitus and Boyer*, 1994]. Numbers at records indicate marine isotope stages (MIS).

duplicate and triplicate analyses of the SST estimates of our samples is 0.3°C (or 0.01 $U^{K'}_{37}$ units). The high sedimentation rates of the sediments result in a rapid removal of the alkenones from the oxic pore water zone with short oxygen-exposure times, unlikely to have caused significant diagenetic alteration of the alkenone-derived SST estimates [*Sinninghe Damsté et al.*, 2002].

[11] Spectral analyses were carried out with the SPECTRUM program [*Schulz and Statteger*, 1997] using a Siegel test to identify significant periodic variations. The level of significance was kept at 0.05, the oversampling factor was set to 4, and the high frequency factor set to 1 in the calculations. Cross-spectral analyses between the signals sharing significant variance in similar frequencies were performed to reveal the coherency of the detected cycles and their phasing. Phase angles are given as lag (up to 180°). The level of significance for the cross-spectral analyses was 0.1, other parameters were the same as for the power spectra calculations. A Welch window and 2 segments with 50% overlap were used. Gaussian-filtering of the records has been performed to investigate changes in the amplitude of the 100-kyr cycle and to isolate the long-term trend from each of the records. The bandwidths of the filters have been adjusted to solely pass the period under consideration and to suppress other orbital frequencies. The used filter characteristics are slightly modified after *Ruddiman et al.* [1989]. The 100-kyr filter has a central frequency of 0.0103 and a bandwidth of 0.002 cycles/kyr. The long-term filter has a central frequency of 0.004 and a bandwidth of 0.004 cycles/kyr.

3. Results

3.1. Tropical Atlantic SST During the MPT

[12] A large temperature range, between 19.5 to 27.6°C, was detected for the ODP Site 1077 SST record for the mid-Pleistocene (Figure 2a), the total amplitude being about 8°C. SSTs are generally lower in glacial than during interglacial stages. The largest absolute temperature change, a warming of 5.8°C, occurred during deglaciation of MIS 22. About 2°C higher SSTs than the modern annual mean (25.8°C, Figure 1), occurred during MIS 15, while lowest SST occurred during MIS 12, 6°C below the modern annual mean. Remarkably, the SST development did not follow the sawtooth-like pattern observed in the record of the benthic oxygen isotopes of Site 677 (Figure 2b); instead the glacials appear as relatively short-lived and sharp drops in SST. On the long-term, a cooling is detected from 1250 kyr BP (MIS 37) to about 930 kyr BP (MIS 25). During MIS 24 and 22, at 925 and at 860 kyr BP respectively, SSTs were as low as during the Last Glacial Maximum (~21°C [*Schneider et al.*, 1995]). SST remained generally low until the end of MIS 22 (at about 860 kyr BP), with a short warming during MIS 23. After MIS 22, a long-term warming is observed, mainly caused by subsequently higher glacial minimum SSTs. This warming trend ends with a strong glacial cooling at the end of MIS 16, at about 640 kyr BP. The following glacial MIS 14 and 12 show a trend to subsequently lower minimum SSTs.

[13] Spectral analysis of the tropical Atlantic SST record reveals strongest power for a 450-kyr cycle (Figure 3a). The length of the SST record, about 800 kyr, is, however, insufficient to attribute a 450-kyr cycle to orbital forcing, but, obviously, this low frequency reflects the long-term trend in the SST record. An 80-kyr cycle contains the second-most power in the SST record. Significant spectral

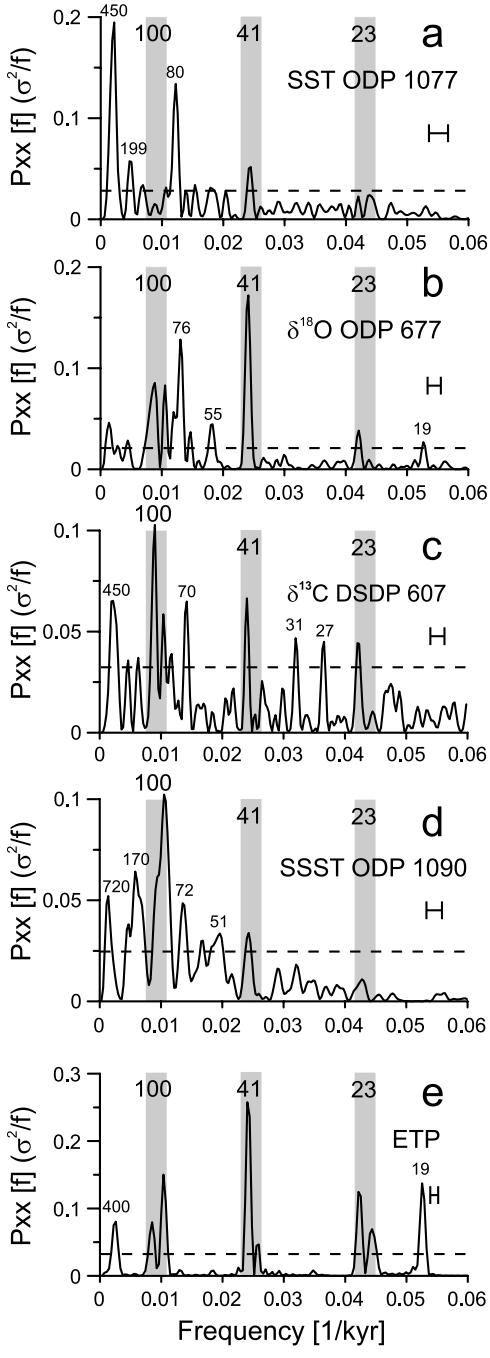

Figure 3. Power spectra of the mid-Pleistocene time series: (a) ODP Site 1077 SST, (b) ODP Site 677 benthic $\delta^{18}O$, (c) DSDP Site 607 benthic $\delta^{13}C$, (d) ODP Site 1090 Subantarctic SSST, and (e) ETP. Small horizontal bars mark 6 dB bandwidths. Dashed lines indicate significance based on a Siegel-test. Orbital frequency bands for eccentricity (100), obliquity (41), and precession (23) are indicated by gray bars. Significant peaks outside the orbital frequency bands are labeled separately.

power also occurs in a 41-kyr cycle. The power of precessional variations is below significance, which may be due to the inaccuracies of the age model.

3.2. The $\delta^{18}O$ Record of Continental Ice Volume

[14] The $\delta^{18}O$ record of benthic foraminifera at ODP Site 677 (Figures 1 and 2b, 01°12′N, 83°44′W, Panama Basin [*Shackleton et al.*, 1990]) has a sufficiently high temporal resolution (average sample spacing = 2.7 kyr) across the mid-Pleistocene and is therefore used as an equivalent to the late Pleistocene SPECMAP ice-volume stack [*Imbrie et al.*, 1989]. Its development differs significantly from the SST record at Site 1077 (Figure 2a). There is no, or only a slight increase in average continental ice volume from MIS 37 to MIS 24. The first significantly higher $\delta^{18}O$ values were abruptly reached during MIS 22, after the main drop in SST during MIS 24. Afterward, the glacial $\delta^{18}O$ values tend to be higher, with most enriched values occurring at the end of MIS 16. A sawtooth-like pattern can be observed in the $\delta^{18}O$ record, most clearly expressed in the glacial MIS 24 and 22, 16 and 12. A long-term reversal, however, like in the SST record from MIS 22 to MIS 16, is not detected, indicating that the long-term warming of the tropical Atlantic Ocean during the MPT was not accompanied by a long-term decrease in continental ice volume.

[15] The ODP Site 677 benthic $\delta^{18}O$ record contains dominant power in the 41-kyr cycle (Figure 3b) in the mid-Pleistocene. Remarkably, a 76-kyr cycle contains the second-most power, possibly related to the 80-kyr cycle found in the tropical SST record. In the eccentricity band, power is present in several frequencies. The low amplitude of the eccentricity-related cycles indicates that the 100-kyr cycle in continental ice-volume variations is not dominant throughout the mid-Pleistocene. Additionally, power in 720-, 55-, 23- and 19-kyr cycles is detected.

3.3. The $\delta^{13}C$ Record of Atlantic Thermohaline Circulation

[16] The $\delta^{13}C$ record of the benthic foraminifer *C. wuellerstorfi* at DSDP Site 607 (Figure 1; 41°00′N, 32°58′W, North Atlantic) is used as proxy for the THC strength in the Atlantic Ocean (Figure 2c) [*Raymo et al.*, 1997; *Ruddiman et al.*, 1989]. The record displays the $\delta^{13}C$ composition of dissolved inorganic carbon ($\delta^{13}C_{DIC}$), primarily determined by the proportions of NADW (North Atlantic Deep Water) and AABW (Antarctic Bottom Water). The mixture of AABW from the south, having relatively low $\delta^{13}C_{DIC}$ values, and NADW from the north, with relatively high $\delta^{13}C_{DIC}$ values, determines the $\delta^{13}C_{DIC}$ and thus the $\delta^{13}C$ of benthic foraminifera [*Kroopnick*, 1985; *Ruddiman et al.*, 1989]. It is therefore implicitly assumed that any changes in preformed $\delta^{13}C_{DIC}$ of NADW and changes in the mean ocean $\delta^{13}C_{DIC}$ were small relative to the variations caused by deepwater circulation changes. The original stratigraphy of DSDP Site 607 [*Ruddiman et al.*, 1989] was adjusted to the stratigraphy of ODP Site 677 by *Raymo et al.* [1997]. The Site 607 benthic $\delta^{13}C$ record (Figure 2c) shows a distinct development during the MPT. $\delta^{13}C$ values are relatively stable from MIS 37 to MIS 25,

with minor brief excursions to more depleted values. At MIS 24, the most pronounced decrease in $\delta^{13}C$ since 3 Ma BP occurred [*Raymo et al.*, 1997]. From this time onward, the $\delta^{13}C$ values were depleted during each glacial stage, but subsequently became more enriched until MIS 14. Toward the end of MIS 12, again very low $\delta^{13}C$ values are detected.

[17] In the power spectrum of the Site 607 benthic $\delta^{13}C$ record (Figure 3c) most power is detected for eccentricity-related cycles. Second-most power is detected for a long-term 450-kyr period and for 70- and 41-kyr cycles. The spectrum of the $\delta^{13}C$ record also shows significant power in 31-, 27- and 23-kyr cycles.

3.4. Southern Ocean Front Positions

[18] The summer sea surface temperature (SSST) record from ODP Site 1090 (Figure 1, 42°55′S, 8°54′E) reflects oceanic front positions in the Subantarctic South Atlantic (Figure 2d [*Becquey and Gersonde*, 2002]). Between 1300 and 400 kyr BP, the SSST record shows increasing glacial-interglacial contrasts. Before 870 kyr BP, only minor SSST variations are detected, ranging between 3 and 6°C. After 870 kyr BP glacial minimum temperatures were lower, corresponding to the temperature range of the present Polar Front. Contemporaneously, interglacial temperatures were higher, reaching present-day values during MIS 13. Since MIS 11, glacial SSST estimates are again higher than during the MPT [*Becquey and Gersonde*, 2002]. Apparently, glacial Southern Ocean fronts were in a generally more northward position in glacials during the MPT than before and afterward.

[19] The SSST record shows dominant power in eccentricity-related cycles (Figure 3d). Second-most power is detected for a 720-kyr long-term period, and 170- and 72-kyr cycles. Small, but significant power is found for 51- and 41-kyr frequencies.

3.5. Orbital Variance

[20] We calculated an artificial record of orbital variance, ETP, containing equal power in all orbital frequencies, i.e., eccentricity (E), obliquity (T) and precession (P) [*Berger and Loutre*, 1991; *Imbrie et al.*, 1984] (Figures 2e and 3e). It is considered to reflect orbital insolation changes. Owing to the amplitude normalization of all orbital frequency bands, ETP contains high-frequency as well as low-frequency variations. High values indicate maximum interglacial forcing. Lowest values are found for MIS 36, 34, 28, 24 to 22, 18, 14 and 12, while highest values occur in MIS 31, 25, 21, 17 and 15.

4. Discussion

4.1. Low-Latitude Insolation

[21] The pattern of the mid-Pleistocene SST development differs significantly from the late Quaternary SST evolution in the tropical Atlantic [*Schneider et al.*, 1995]. Instead of predominant 100- and 23-kyr cycles, a dominance of obliquity and nonorbital cycles is detected (Figure 3a). These results rule out that tropical Atlantic SSTs were directly controlled by low-latitude insolation during the mid-Pleistocene, since the low-latitude insolation signal contains no 41- and 80-kyr variability [*Berger and Loutre*, 1991]. Our findings are supported by a SST record from the equatorial Pacific, suggesting that tropical SST in the early to mid-Pleistocene varied independently from low-latitude insolation [*Liu and Herbert*, 2004]. Instead, it was inferred that climatic coupling between low and high latitudes was tighter under smaller ice sheet conditions [*Liu and Herbert*, 2004]. In the low latitudes, there is apparently a fundamental difference between the tropical SST response to orbital insolation during the mid-Pleistocene and the late Quaternary.

4.2. Precession

[22] Assessing the influence of precessional-driven insolation changes on the mid-Pleistocene tropical SST evolution is difficult because spectral analysis of the ODP Site 1077 SST record (Figure 3a) yields no significant precessional power. Possibly, the inaccuracy of the age model of ODP Site 1077 for the mid-Pleistocene [*Dupont et al.*, 2001] results in the low precessional power of the spectral analysis. Visual inspection of the SST record (Figure 2a), however, reveals high-frequency variations, which were most probably related to precessional forcing. Interestingly, the most pronounced decreases in the tropical SST record, i.e., in MIS 30, 24, 16, and 14, seem to have occurred right after peaks of highest ETP values (Figures 2a and 2e). These high peaks in the ETP record are precessional minima co-occurring with maxima of eccentricity or obliquity. About 9 to 12 kyr after precessional maxima, boreal summer insolation was lowest, causing strong wind-driven upwelling in the Angola Basin. Consequently, the strong decreases in the tropical SST record shortly after high ETP values were likely related to precessional-forced upwelling. This indicates that low-latitude insolation-driven processes, although weaker than during the late Quaternary, may have influenced the tropical SST development during the MPT.

4.3. Obliquity

[23] All investigated time series contain significant variance in the 41-kyr obliquity cycle (Figure 3). Cross-spectral analyses show that all records are coherent in the 41-kyr frequency band (Table 1). The obliquity-related variations in the tropical SST record (ODP 1077) consistently follow the changes in the Earth's tilt by 5.5 kyr during the mid-Pleistocene, in phase with frontal movements in the Southern Ocean (ODP 1090) (Figure 4). The continental ice-volume variations (ODP 677) lag maximum tilt by about 8.9 kyr (Figure 4, Table 1), in agreement with the time lag of 8.0 kyr assigned by orbital tuning [*Imbrie et al.*, 1984; *Shackleton et al.*, 1990], while the Site 607 $\delta^{13}C$ record shows a considerably larger phase lag of about 12.9 kyr relative to obliquity-related insolation changes (Figure 4, Table 1). Strongest NADW-formation was thus established significantly later than full interglacial conditions in the obliquity cycle. Cross-checking the obliquity phasing of the ODP 677 $\delta^{18}O$ record against the SST changes in the tropical Atlantic reveals a lead of SST by about 3.2 ± 1.0 kyr (Table 1).

[24] The phase angles for mid-Pleistocene SST variations offshore Angola, in the southern Indian Ocean and the Subantarctic South Atlantic are similar to those in the late Quaternary (Table 1), suggesting that the same mechanism

Table 1. Phase Angles in the Obliquity (41 kyr) Cycle[a]

Time Series	Coherency	Nonzero Coherency (80%)	Phase Angle, deg.	Time Lag, kyr
		Mid-Pleistocene Versus ETP		
ODP 1077 SST	0.99	0.96	48 ± 6	5.5 ± 0.7
ODP 1090 SSST	0.99	0.96	52 ± 4	5.9 ± 0.5
ODP 677 $-\delta^{18}O_{bent.}$	0.99	0.96	78 ± 5	8.9 ± 0.6
DSDP 607 $\delta^{13}C_{wuell.}$	0.97	0.96	113 ± 9	12.9 ± 1.0
		Versus $\delta^{18}O_{677}$		
ODP 1077 SST	0.99	0.96	−29 ± 8	−3.2 ± 1.0
		Late Quaternary Versus Minimum Ice		
GeoB 1016 SST Angola margin	0.76	0.64	−28 ± 20	−3.2 ± 2.3
E45-29/E49-18 SST South Indian fronts	0.86	0.65	−27 ± 15	−3.1 ± 1.7
PS2082-1 SST South Atlantic fronts	0.92	0.73	−18 ± 12	−2.1 ± 1.4
PS2489-2 SSST South Atlantic fronts	0.82	0.80	−13 ± 15	−1.5 ± 1.7

[a]ETP describes summed orbital variance following the convention by *Imbrie et al.* [1989] using the data of *Berger and Loutre* [1991]. ODP 1090 SSST data are from *Becquey and Gersonde* [2002], data of ODP 677 $\delta^{18}O$ are from *Shackleton et al.* [1990], data of DSDP 607 $\delta^{13}C$ are from *Ruddiman et al.* [1989] with the stratigraphy of *Raymo et al.* [1997]. Results for the late Quaternary are taken from the literature. Data of GeoB 1016 (11°46′S, 11°41′E) are from *Schneider et al.* [1995], data for E45-29 (44°53′S, 106°31′E) and E49-18 (46°03′S, 90°10′E) are from *Howard and Prell* [1992], PS2082-1 (43°13′S, 11°44′E) data are from *Brathauer and Abelmann* [1999], and PS2489-2 (42°52′S, 8°58′E) data are from *Becquey and Gersonde* [2003]. All late Quaternary records are crossed with the inverse SPECMAP record [*Imbrie et al.*, 1984], except for PS2489-2 SSST, which is crossed with benthic foraminiferal $\delta^{18}O$ of that core [*Becquey and Gersonde*, 2003]. A negative phase lag represents a lead.

was responsible for obliquity-related SST variations in the tropical Atlantic during the mid-Pleistocene and the late Quaternary. The SST records from the Subantarctic South Atlantic reflect past oceanic front positions [*Becquey and Gersonde*, 2003; *Brathauer and Abelmann*, 1999; *Howard and Prell*, 1992]. Their changes thus indicate variations in the meridional thermal gradient of the South Atlantic Ocean. As in the late Quaternary, northward shifts in the subtropical front simultaneously increase the zonal strength of the SE trade winds, enhancing upwelling in the Angola Basin. They also reduce the inflow of warm Indian Ocean surface waters into the South Atlantic via the Agulhas leakage, leading to a larger inflow of colder waters from the South Atlantic Current and the Circum-Antarctic Current [*Schneider et al.*, 1996]. The Southern Ocean frontal positions, in turn, are strongly linked to the sea-ice extent in the Subantarctic South Atlantic [*Imbrie et al.*, 1993]. The sea-ice extent and oceanic front positions, reflected by the Southern Ocean SST, are obviously very sensitive to changes in Southern Hemisphere insolation changes indicated by their lead of about 3 kyr over continental ice-volume variations (Table 1). Sea ice is not reflected in the benthic $\delta^{18}O$ record, which mainly reflects continental ice volume. The tropical Atlantic SST variations in the obliquity cycle were apparently ultimately linked to changes in Subantarctic sea-ice extent. The main driver for obliquity-related SST changes in the tropical Atlantic were thus insolation changes in the high-latitude Southern Hemisphere, controlling the Subantarctic sea-ice extent.

4.4. The 100-kyr Cycle

[25] The 100-kyr cyclicity in the continental ice-volume variations increased during the MPT [*Mudelsee and Schulz*, 1997; *Prell*, 1982]. To investigate the 100-kyr amplitude variations in the mid-Pleistocene records, we compare their 100-kyr filtered signals (Figure 5). All filtered signals, except the orbital forcing, show increasing amplitudes toward the end of the MPT. After 650 kyr BP, the amplitude of the filtered tropical SST variations became significantly larger than the envelope of the variations before (Figure 5a). Also the filtered continental ice volume (Figure 5b) and Atlantic THC signals (Figure 5c) increased in amplitude at approximately the same time. Only the 100-kyr variability of the Subantarctic SSST increased already about 100 kyr earlier (Figure 5d). The coherent increase in eccentricity-related power in the tropical SST and the high-latitude continental ice volume indicates that the SSTs and the ice volume did not change independently of one another.

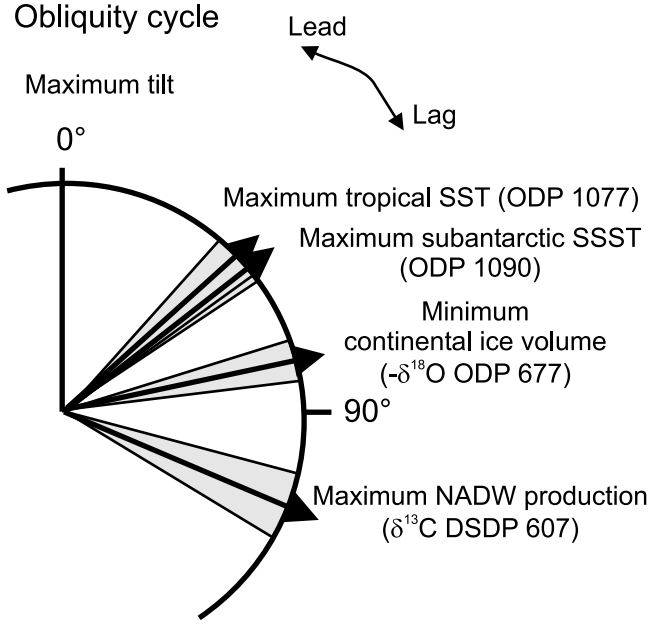

Figure 4. Phase relations in the obliquity cycle shown in a phase wheel: maximum obliquity/tilt is at 0°, a phase lag is clockwise. The shaded areas indicate the error estimates of the phase angles.

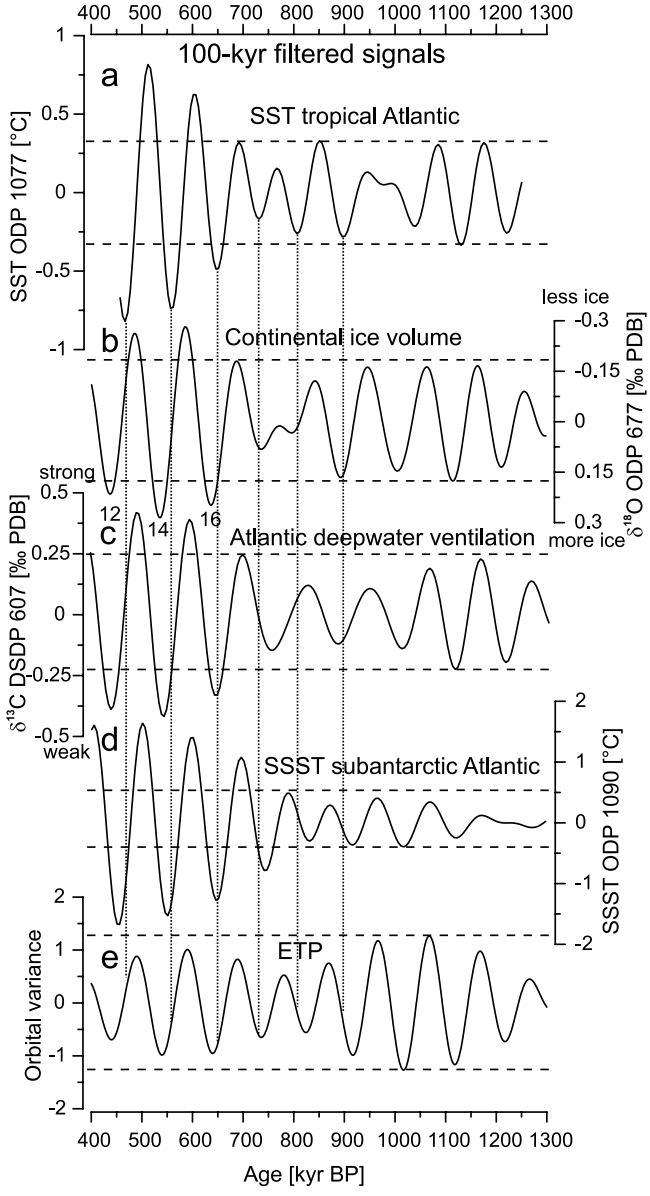

Figure 5. Amplitudes of the 100-kyr variations in the investigated time series obtained by Gaussian-filtering (central frequency: 0.0103 cycles/kyr, bandwidth: 0.002cycles/kyr): (a) ODP Site 1077 SST, (b) ODP Site 677 benthic $\delta^{18}O$ (note axis orientation), (c) DSDP Site 607 benthic $\delta^{13}C$, (d) ODP Site 1090 Subantarctic SSST, and (e) ETP. The horizontal broken lines are the envelope of 100-kyr variations before the mid-Pleistocene increase of 100-kyr power in each time series. Numbers in Figure 5b indicate marine isotope stages.

[26] The cross-spectral analyses in the eccentricity band were restricted to the time interval from 900 to 450 kyr BP because the 100-kyr power in the signals is low in the older part of the records (Table 2). The order of events observed in the 100-kyr cycle is: (1) maximum tropical SSTs and maximum Subantarctic SSSTs, (2) maximum strength of the Atlantic THC, (3) minimum continental ice volume. Like in the obliquity cycle, the tropical SST variations in the eccentricity band were in phase with the frontal movements in the Southern Ocean and preceded the continental ice volume. In the late Quaternary, eccentricity-related SST variations in the tropical Atlantic occurred, on average, 3.9 kyr before continental ice-volume changes (Table 2) [*Schneider et al.*, 1996], in phase with movements of the Subantarctic fronts in the southern Indian Ocean and the South Atlantic [*Becquey and Gersonde*, 2003; *Brathauer and Abelmann*, 1999; *Howard and Prell*, 1992]. As for the obliquity cycle, this phasing indicates a dominant control of mid-Pleistocene eccentricity-related SST variations in the equatorial Atlantic by changes in the Southern Hemisphere thermal gradient due to movements of Subantarctic Southern Ocean fronts. The simultaneous increase in 100-kyr variability in the tropical SST and benthic $\delta^{18}O$ records, however, also suggests a strong influence of continental ice volume on the tropical Atlantic SST evolution. This influence came, most likely, from the continental ice volume predetermining the main cyclicity of Subantarctic sea-ice variations and the oceanic front positions. The high-latitude sea-ice extension is thought to play a key role in the climatic evolution of the 100-kyr ice-volume cycles [*Gildor and Tziperman*, 2000; *Kravtsov and Dewar*, 2003; *Tziperman and Gildor*, 2003]. The general rhythm of sea-ice variations was obviously determined by the continental ice-volume changes, whereas the early response of the Subantarctic sea ice was driven by Southern Hemisphere insolation changes. An early reduction in sea-ice extent may be the driver for the deglacial atmospheric CO_2 rise [*Stephens and Keeling*, 2000], preceding continental ice-volume changes [*Mudelsee*, 2001; *Shackleton*, 2000]. Another feedback for deglaciation may have been the early opening of the Agulhas leakage, which was inferred to lead to resumption of the Atlantic THC [*Knorr and Lohmann*, 2003]. Variations in the strength of the THC preceded continental ice-volume changes in the 100-kyr cycle (Table 2), contrary to the phasing in the 41-kyr cycle (Table 1). Apparently, the establishment of the 100-kyr cycle in continental ice-volume variations has increased the role of the THC as an important feedback mechanism for deglaciation.

[27] A detailed visual inspection of the 100-kyr variations reveals that toward the end of the mid-Pleistocene, tropical SST changes in the 100-kyr cycle occurred even before frontal movements in the Southern Ocean (compare vertical lines in Figure 5). The Site 1077 100-kyr SST variations followed the Site 1090 100-kyr SSST variations before 650 kyr BP and lead afterward (Figures 5a and 5d). Consequently, an additional process must have been involved during the large 100-kyr glaciations, which caused warming of the eastern tropical Atlantic during times of largest continental ice volume. Reductions of the THC are not a likely candidate, since Site 607 benthic $\delta^{13}C$ changes lag tropical SST changes in the eccentricity cycle (Figures 5a and 5c). Enhanced return flow of warm Western Atlantic waters, however, driven by strong SE trade winds, as currently observed during austral winter [*Philander and Pacanowski*, 1986], would be able to warm the eastern tropical Atlantic during times of largest ice volume. The strongest trade winds were coupled to the largest ice volume

Table 2. Phase Angles in the Eccentricity (100 kyr) Cycle From 900 to 450 kyr BP[a]

Time Series	Coherency	Nonzero Coherency (80%)	Phase Angle, deg.	Time Lag, kyr
		Mid-Pleistocene Versus ETP		
ODP 1090 SSST	0.99	0.96	−10 ± 3	−2.8 ± 0.8
ODP 1077 SST	0.96	0.96	−8 ± 10	−2.2 ± 2.8
DSDP 607 $\delta^{13}C_{wuell.}$	0.93	0.96	5 ± 14	1.4 ± 3.9
ODP 677 $-\delta^{18}O_{bent.}$	0.98	0.96	24 ± 8	6.7 ± 2.2
		Versus $\delta^{18}O_{677}$		
ODP 1077 SST	0.91	0.96	−31 ± 16	−8.6 ± 4.4
		Late Quaternary Versus Minimum Ice		
GeoB 1016 SST Angola margin	0.92	0.64	−14 ± 15	−3.9 ± 4.2
E45-29/E49-18 SST South Indian fronts	0.81	0.65	−18 ± 18	−5.0 ± 5.0
PS2082-1 SST South Atlantic fronts	0.97	0.73	−18 ± 6	−5.0 ± 1.7
PS2489-2 SSST South Atlantic fronts	0.93	0.80	−23 ± 8	−6.4 ± 2.2

[a]See Table 1 for notes.

and sea-ice extent, which explains why their warming effect on the eastern tropical Atlantic only occurred after the onset of the enlarged 100-kyr variations in continental ice volume. In the large-amplitude 100-kyr glaciations after the MPT, the effects of late glacial warming due to strongest trade winds and early deglacial warming due to changes in the positions of the South Atlantic front positions thus combined, resulting in an even larger temporal lead of tropical Atlantic SST over continental ice-volume changes (Table 2).

4.5. The 80-kyr Variations

[28] During the mid-Pleistocene transition, some spectral power is observed in 76- to 80-kyr cycles. It is prominent in the tropical Atlantic SST record (Figure 3a) and has also been found in benthic $\delta^{18}O$ records from various locations [*Mudelsee and Schulz*, 1997]. While some authors have explained it as a doubling of the 41-kyr cycle [*Berger et al.*, 1998], others attribute it to premature calving events of the enlarged ice sheets during the transition from a 41-kyr to a 100-kyr cyclicity [*Mudelsee and Schulz*, 1997]. To gain more insight into their phasing, we conducted cross-spectral analyses between the available records (Table 3). ETP contains no power in an 80-kyr cycle, so the SST record was chosen as cross-spectral reference. Within error limits, the 76- to 80-kyr cycles were in phase in all records (Table 3). In contrast to the results from the phase analyses in the 41- and 100-kyr cycles, in which tropical SST variations significantly preceded continental ice-volume changes, no such early response is detected for the 80-kyr cycle, indicating that no orbital forcing was involved. This result suggests that the 80-kyr SST cycles were directly caused by variations in continental ice volume during the MPT. Most probably, the transitional occurrence of the 80-kyr cycle was an immediate response on premature calving events related to the growth of the continental ice sheets during the MPT [*Mudelsee and Schulz*, 1997].

4.6. Long-Term Evolution

[29] The long-term trend of the Site 1077 SST record (Figure 6a) explains a significant portion of the signal, about 3°C. From 1200 to about 1000 kyr BP, long-term tropical SSTs were high, with a slight decrease at 1100 kyr BP. A distinct minimum occurred at around 900 kyr BP, followed by an increase lasting until 600 kyr BP. The long-term increase from 900 to 600 kyr BP was mainly caused by subsequently higher glacial SSTs. During the glacial MIS 14, around 550 kyr BP, the glacial minimum SST decreased again and the long-term tropical warming ended (Figure 6a). This long-term development differs significantly from the long-term evolution of continental ice volume (Figure 6b) and orbital insolation (Figure 6e). The continental ice volume (Figure 6b) also reached a maximum at 900 kyr BP, coinciding with the SST minimum. A second, even stronger maximum of continental ice volume at 650 kyr BP, however, is not reflected as a minimum in the long-term SST record. This excludes the continental ice volume as direct forcing of the long-term tropical SST evolution during the MPT. The long-term minimum of orbital insolation, reflected by ETP, was centered at 800 kyr BP, 100 kyr after the SST minimum. Therefore also direct orbital insolation forcing cannot explain the long-term SST development. Instead, a mechanism must be responsible that warms the tropical surface waters of the Atlantic during increased mean continental ice volume, which is independent of orbital insolation.

[30] Reductions in the THC can lead to surface water warming in the tropical and South Atlantic Ocean by the "bipolar seesaw" mechanism [*Crowley*, 1992]. This process has only been inferred for short-term climatic events [*Manabe and Stouffer*, 1997; *Rühlemann et al.*, 1999]. The deep ventilation of the Atlantic Ocean was indeed severely weakened during the MPT. The long-term decline of about 0.8‰ in the Site 607 benthic $\delta^{13}C$ record (Figure 6c) is much larger than the inferred mean ocean $\delta^{13}C_{DIC}$ change of about 0.3‰ during the MPT [*Raymo et al.*, 1997]. Consequently, it primarily reflects a change in

Table 3. Phase Angles in the 80-kyr Cycle[a]

Time Series	Coherency	Nonzero Coherency (80%)	Phase Angel, deg.	Lag, kyr
		Versus ODP 1077 SST		
ODP 1090 SSST	0.71	0.96	−25 ± 32	−5.6 ± 7.1
ODP 677 $-\delta^{18}O_{bent.}$	0.83	0.96	−1 ± 23	−0.2 ± 5.1
DSDP 607 $\delta^{13}C_{wuell.}$	0.92	0.96	10 ± 15	2.2 ± 3.3

[a]See Table 1 for notes.

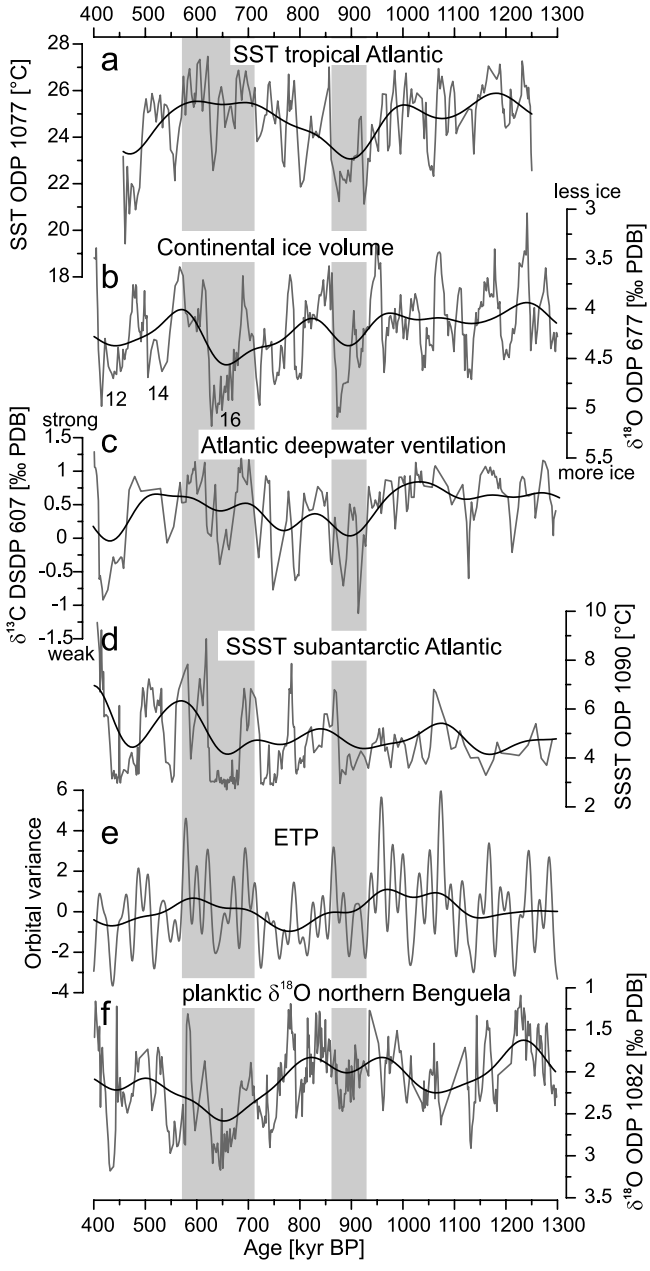

Figure 6. The long-term trends of investigated mid-Pleistocene time series obtained by Gaussian-filtering (central frequency: 0.004 cycles/kyr, bandwidth: 0.004 cycles/kyr): (a) ODP Site 1077 SST, (b) ODP Site 677 benthic $\delta^{18}O$ (note axis orientation), (c) DSDP Site 607 benthic $\delta^{13}C$, (d) ODP Site 1090 Subantarctic SSST, (e) ETP, and (f) the $\delta^{18}O$ of planktonic foraminifera from ODP Site 1082 (northern Benguela upwelling region [*Jahn et al.*, 2003]). Numbers in Figure 6b indicate marine isotope stages.

the Atlantic deepwater ventilation. A long-term minimum of carbonate deposition in the South Atlantic confirms the reduced Atlantic deep ventilation and stronger influence of more aggressive, southern source deep waters during the MPT [*Schmieder et al.*, 2000]. The long-term trend in the Site 607 benthic $\delta^{13}C$ record shows a similar development during the mid-Pleistocene as the tropical Atlantic SST record (Figure 6c). The tropical and South Atlantic surface waters, however, should have warmed up most when Atlantic THC was most reduced. Instead, rather the opposite is observed (Figures 6a and 6c). Thus the long-term reduction of the Atlantic THC cannot have caused the long-term tropical warming during the MPT.

[31] Therefore we suggest another cause for the long-term warming of the tropical Atlantic Ocean during the MPT. The long-term development of the Site 1090 SSST record (Figure 6d) shows a cooling from 840 to 660 kyr BP, reflecting on average northward displaced frontal positions in the Southern Ocean during glacials [*Becquey and Gersonde*, 2002]. The northward displaced Subantarctic fronts reduced the inflow of warm Indian Ocean waters into the Atlantic and led to a steeper meridional thermal gradient in the South Atlantic during the mid-Pleistocene glacials, leading to enhanced upwelling. Combined, these processes would lead to a cooling in the South Atlantic. However, simultaneously, the stronger SE trade winds would have also led to a larger surface water mass transport from the eastern South Atlantic into the tropical western Atlantic, which would have resulted into a stronger backflow of warm surface waters into the tropical eastern Atlantic [*Philander and Pacanowski*, 1986], as inferred for the warming of the tropical eastern Atlantic during full glacial conditions in the 100-kyr cycle (see above). Supporting evidence for this mechanism comes from a planktonic $\delta^{18}O$ record from the northern Benguela upwelling region (ODP Site 1082, 21.5°S, 11.5°E, Figure 6f) [*Jahn et al.*, 2003]. This record contains a mixture of the continental ice volume and local temperature signals. Remarkably, it shows a long-term increase of planktonic $\delta^{18}O$ from 830 to 660 kyr BP. This increase was caused partly by the increase in continental ice mass (compare with Figure 6c) and partly by stronger upwelling, corroborated by high values of total organic carbon accumulation at Site 1082 [*Jahn et al.*, 2003]. This evidence confirms that SE trade winds indeed were strongest in the mid-Pleistocene glacials, causing strong upwelling in the northern Benguela region and, presumably, strong return flow of warm tropical waters from the western Atlantic into the eastern tropical Atlantic. The long-term tropical warming during the MPT was thus most likely caused by the extremely northward displaced Southern Ocean fronts during the mid-Pleistocene glacials. Apparently, the Southern Hemisphere frontal positions, linked to the Subantarctic sea-ice extent, play the key role for the anomalous tropical SST development during the MPT. We suggest that the long-term tropical warming during the MPT was causally linked to the evolution of the continental ice volume. It started after the growth of additional continental ice mass around 900 kyr BP and ended with the establishment of the 100-kyr cycle in ice-volume variations at about 650 kyr BP. We speculate that the enlarged continental ice mass after 900 kyr BP was not in a stable configuration before 650 kyr BP, and that the climate system adjusted to the new boundary conditions with the amplification of the 100-kyr cycle. The long-term tropical warming thus likely

formed an important feedback mechanism promoting the transition to the new main global climatic cyclicity.

5. Conclusions

[32] We detect a distinct mid-Pleistocene SST evolution in the eastern tropical Atlantic. The start of the mid-Pleistocene transition (MPT) is marked by a strong tropical cooling, contemporary to the growth of additional mean continental ice mass. During the mid-Pleistocene, SST variations in the tropical Atlantic show prevalent 41-kyr cycles. The amplitude of 100-kyr SST variability increased at 650 kyr BP, coinciding with the establishment of 100-kyr variations in continental ice volume changes. The tropical SST variations thus generally followed the pattern of global climatic changes driven by the continental ice sheets, and were not directly forced by low-latitude insolation changes. In the 41- and 100-kyr cycles, however, tropical SST changes preceded continental ice-volume variations, but were in-phase with or leading over frontal movements in the Southern Ocean. Frontal positions in the high-latitude South Atlantic are determined by the extent of Subantarctic sea ice, which is apparently highly sensitive to Southern Hemisphere insolation changes. Southern Ocean frontal positions determine the thermal gradient of the South Atlantic, modulating strength and zonality of the SE trade winds and, thus, the intensity of wind-driven equatorial upwelling. Simultaneously, the position of the South Atlantic subtropical front controls the advection of warm Indian Ocean waters into the South Atlantic. After the establishment of large 100-kyr SST cycles, the eastern tropical Atlantic warmed during full glacial conditions before Southern Ocean frontal movements. This is attributed to a strengthened return flow of warm surface waters from the western into the eastern tropical Atlantic driven by strong SE trade winds. The early tropical SST changes underline the role of the tropics as an important amplifier of orbital-driven climate changes. During the mid-Pleistocene, tropical SST variations show a strong 80-kyr cycle, in-phase with transitional continental ice-volume changes. This cycle is absent in the orbital insolation and was thus likely directly forced by premature calving events of the enlarged continental ice sheets during the MPT. A prominent long-term warming of the eastern tropical Atlantic occurred during the MPT, mainly due to subsequently increased glacial minimum temperatures. The tropical warming started with the growth of additional mean continental ice mass around 900 kyr BP and ended with the establishment of the 100-kyr cycle around 650 kyr BP. During the MPT glacials, the Southern Ocean fronts were in extremely northern positions, causing intensified SE trade winds and, in turn, a strongly enhanced return flow of warm waters from the western into the eastern tropical Atlantic. While, apparently, the MPT was initially caused by the change in mean state and frequency of the continental ice volume variations, the changes in sea-ice extent around Antarctica and the associated frontal movements in the Southern Ocean were the main forcing mechanisms of the mid-Pleistocene development of the tropical Atlantic SSTs.

[33] **Acknowledgments.** We appreciate the comments of an anonymous reviewer, which helped to improve the manuscript. We thank Ralph Schneider (University of Bordeaux) for discussions. We thank Lydie Dupont (University of Bremen) and Lucas Lourens (University of Utrecht) for help with the stratigraphy. We gratefully thank the Ocean Drilling Program (ODP) for the supply of samples. The Dutch scientific funding organization (NWO) is thanked for financial support (project 75019617).

References

Becquey, S., and R. Gersonde (2002), Past hydrographic and climatic changes in the Subantarctic zone of the South Atlantic—The Pleistocene record from ODP Site 1090, *Palaeogeogr. Palaeoclimatol. Palaeoecol.*, *182*, 221–239.

Becquey, S., and R. Gersonde (2003), A 0.55-Ma paleotemperature record from the Subantarctic zone: Implications for Antarctic Circumpolar Current development, *Paleoceanography*, *18*(1), 1014, doi:10.1029/2000PA000576.

Berger, A., and M. F. Loutre (1991), Insolation values for the climate of the last 10 million years, *Quat. Sci. Rev.*, *10*, 297–317.

Berger, W. H., and E. Jansen (1994), Mid-Pleistocene climate shift—The Nansen connection, in *The Polar Oceans and Their Role in Shaping the Global Environment*, *Geophys. Monogr.*, vol. 85, edited by O. M. Johannessen R. D. Muench and J. E. Overland, pp. 295–311, AGU, Washington, D. C.

Berger, W. H., G. Wefer, C. Richter, and the Shipboard Scientific Party (1998), Color cycles in Quaternary sediments from the Congo fan region (Site 1075): A statistical analysis, *Proc. Ocean Drill. Program Initial Rep.*, *175*, 561–567.

Bolton, E. W., K. A. Maasch, and J. M. Lilly (1995), A wavelet analysis of Plio-Pleistocene climate indicators: A new view of periodicity evolution, *Geophys. Res. Lett.*, *22*, 2753–2756.

Brassell, S. C., G. Eglinton, I. T. Marlowe, U. Pflaumann, and M. Sarnthein (1986), Molecular stratigraphy: A new tool for climatic assessment, *Nature*, *320*, 129–133.

Brathauer, U., and A. Abelmann (1999), Late Quaternary variations in sea surface temperatures and their relationship to orbital forcing recorded in the Southern Ocean (Atlantic sector), *Paleoceanography*, *14*, 135–148.

Crowley, T. J. (1992), North Atlantic deep water cools the Southern Hemisphere, *Paleoceanography*, *7*, 489–497.

de Leeuw, J. W., F. W. van der Meer, W. I. C. Rijpstra, and P. A. Schenck (1980), On the occurrence and structural identification of long-chain unsaturated ketones and hydrocarbons in sediments, in *Advances in Organic Geochemistry 1979*, edited by A. G. Douglas and J. R. Maxwell, pp. 211–217, Elsevier, New York.

de Menocal, P. B., and D. Rind (1993), Sensitivity of Asian and African climate to variations in seasonal insolation, glacial ice cover, sea surface temperature, and Asian orography, *J. Geophys. Res.*, *98*, 7265–7287.

Dupont, L. M., B. Donner, R. R. Schneider, and G. Wefer (2001), Mid-Pleistocene environmental change in tropical Africa began as early as 1.05 Ma, *Geology*, *29*, 195–198.

Eisma, D., and A. J. van Bennekom (1978), The Zaire river and estuary and the Zaire outflow in the Atlantic Ocean, *Neth. J. Sea Res.*, *12*, 255–272.

Gildor, H., and E. Tziperman (2000), Sea ice as the glacial cycles' climate switch: Role of seasonal and orbital forcing, *Paleoceanography*, *15*, 605–615.

Howard, W. R., and W. L. Prell (1992), Late Quaternary surface circulation of the southern Indian Ocean and its relationship to orbital variations, *Paleoceanography*, *7*, 79–118.

Hsü, C.-P. F., and J. M. Wallace (1976), The global distribution of the annual and semiannual cycles in precipitation, *Mon. Weather Rev.*, *104*, 1093–1101.

Imbrie, J., J. D. Hays, D. G. Martinson, A. McIntyre, A. C. Mix, J. J. Morley, N. G. Pisias, W. L. Prell, and N. J. Shackleton (1984), The orbital theory of Pleistocene climate: Support from a revised chronology of the marine $\delta^{18}O$ record, in *Milankovitch and Climate, Understanding the Response to Astronomical Forcing*, edited by A. Berger et al., pp. 269–305, Springer, New York.

Imbrie, J., A. McIntyre, and A. Mix (1989), Oceanic response to orbital forcing in the late Quaternary: Observational and experimental strategies, in *Climate and Geo-sciences*, edited by A. Berger, S. Schneider, and J. C. Duplessy, pp. 121–164, Springer, New York.

Imbrie, J., et al. (1993), On the structure and origin of major glaciation cycles: 2. The

100,000-year cycle, *Paleoceanography*, *8*, 699–735.

Jahn, B., B. Donner, P. J. Müller, U. Röhl, R. R. Schneider, and G. Wefer (2003), Pleistocene variations in dust input and marine productivity in the northern Benguela Current: Evidence of evolution of global glacial-interglacial cycles, *Palaeogeogr. Palaeoclimatol. Palaeoecol.*, *193*, 515–533.

Jansen, J. H. F., and L. M. Dupont (2001), A revised composite depth record for site 1077 based on magnetic susceptibility and XRF core scanner (CORTEX) data, *Proc. Ocean Drill. Program Sci. Results*, *175*. (Available at http://www-odp.tamu.edu/publications/175_SR/VOLUME/CHAPTERS/SR175_20.PDF.)

Jansen, J. H. F., T. C. E. Van Weering, R. Gieles, and J. Van Iperen (1984), Middle and late Quaternary oceanography and climatology of the Zaire-Congo fan and adjacent eastern Angola Basin, *Neth. J. Sea Res.*, *17*, 201–249.

Jansen, J. H. F., E. Ufkes, and R. R. Schneider (1996), Late Quaternary movements of the Angola-Benguela Front, SE Atlantic, and implications for advection in the equatorial Ocean, in *The South Atlantic*, edited by G. Wefer et al., pp. 553–575, Springer, New York.

Katz, E. J., and S. L. Garzoli (1982), Response of the western equatorial Atlantic Ocean to an annual wind cycle, *J. Mar. Res.*, *40*, 307–327.

Kim, J.-H., R. R. Schneider, S. Mulitza, and P. J. Müller (2003), Reconstruction of SE trade-wind intensity based on sea-surface temperature gradients in the Southeast Atlantic over the last 25 kyr, *Geophys. Res. Lett.*, *30*(22), 2144, doi:10.1029/2003GL017557.

Knorr, G., and G. Lohmann (2003), Southern Ocean origin for the resumption of Atlantic thermohaline circulation during deglaciation, *Nature*, *424*, 532–536.

Kravtsov, S., and W. K. Dewar (2003), On the role of thermohaline advection and sea ice in glacial transitions, *J. Geophys. Res.*, *108*(C6), 3203, doi:10.1029/2002JC001439.

Kroopnick, P. M. (1985), The distribution of ^{13}C of CO_2 in the world oceans, *Deep Sea Res.*, *32*, 57–84.

Lau, K.-M., and H. Weng (1995), Climate signal detection using wavelet transform: How to make a time series sing, *Bull. Am. Meteorol. Soc.*, *76*, 2391–2402.

Levitus, S., and T. P. Boyer (1994), *World Ocean Atlas 1994*, vol. 4, *Temperature, NOAA Atlas NESDIS 4*, 99 pp., U.S. Dept. of Comm., Washington, D. C.

Liu, Z., and T. D. Herbert (2004), High-latitude influence on the eastern equatorial Pacific climate in the early Pleistocene epoch, *Nature*, *427*, 720–723.

Lutjeharms, J. R. E., and R. C. van Ballegooyen (1988), The retroflection of the Agulhas Current, *J. Phys. Oceanogr.*, *18*, 1570–1583.

Maasch, K. A. (1988), Statistical detection of the mid-Pleistocene transition, *Clim. Dyn.*, *2*, 133–143.

Manabe, S., and A. J. Broccoli (1985), The influence of continental ice sheets on the climate of an ice age, *J. Geophys. Res.*, *90*, 2167–2190.

Manabe, S., and R. Stouffer (1997), Coupled ocean-atmosphere model response to freshwater input: Comparison to Younger Dryas event, *Paleoceanography*, *12*, 321–336.

McIntyre, A., W. F. Ruddiman, K. Karlin, and A. C. Mix (1989), Surface water response of the equatorial Atlantic Ocean to orbital forcing, *Paleoceanography*, *4*, 19–55.

Meeuwis, J. M., and J. R. E. Lutjeharms (1990), Surface thermal characteristics of the Angola-Benguela Front, *S. Afr. J. Mar. Sci.*, *9*, 261–279.

Mix, A. C., W. F. Ruddiman, and A. McIntyre (1986), Late Quaternary paleoceanography of the tropical Atlantic: 1. Spatial variability of annual sea surface temperatures, 0–20,000 years B. P., *Paleoceanography*, *1*, 43–66.

Mudelsee, M. (2001), The phase relations among atmospheric CO_2 content, temperature and global ice volume over the past 420 ka, *Quat. Sci. Rev.*, *20*, 583–589.

Mudelsee, M., and M. Schulz (1997), The mid-Pleistocene climate transition: Onset of 100 ka cycle lags ice volume build-up by 280 ka, *Earth Planet. Sci. Lett.*, *151*, 117–123.

Müller, P. J., G. Kirst, G. Ruhland, I. von Storch, and A. Rosell-Mele (1998), Calibration of the alkenone paleotemperature index $U^{K'}_{37}$ based on core-tops from the eastern South Atlantic and the global ocean (60°N-60°S), *Geochim. Cosmochim. Acta*, *62*, 1757–1772.

Park, J., and K. A. Maasch (1993), Plio-Pleistocene time evolution of the 100–kyr cycle in marine paleoclimate records, *J. Geophys. Res.*, *98*, 447–461.

Peterson, R. G., and L. Stramma (1991), Upper-level circulation in the South Atlantic Ocean, *Progr. Oceanogr.*, *26*, 1–73.

Philander, S. G. H., and R. C. Pacanowski (1986), A model of the seasonal cycle in the tropical Atlantic Ocean, *J. Geophys. Res.*, *91*, 14,192–14,206.

Pisias, N. G., and T. C. J. Moore (1981), The evolution of Pleistocene climate: A time series approach, *Earth Planet. Sci. Lett.*, *52*, 450–458.

Prahl, F. G., and S. G. Wakeham (1987), Calibration of unsaturation patterns in long-chain ketone compositions for palaeotemperature assessment, *Nature*, *330*, 367–369.

Prell, W. L. (1982), Oxygen and carbon isotope stratigraphy for the Quaternary of hole 502B: Evidence for two modes of isotopic variability, *Proc. Deep Sea Drill. Program Initial Rep.*, *68*, 455–464.

Rau, A. J., J. Rogers, J. R. E. Lutjeharms, J. Giraudeau, J. A. Lee-Thorp, M.-T. Chen, and C. Waelbroeck (2002), A 450-kyr record of hydrological conditions on the western Agulhas Bank slope, south of Africa, *Mar. Geol.*, *180*, 183–201.

Raymo, M. E., D. W. Oppo, and W. Curry (1997), The mid-Pleistocene climate transition: A deep sea carbon isotopic perspective, *Paleoceanography*, *12*, 546–559.

Ruddiman, W. F., M. E. Raymo, D. G. Martinson, B. M. Clement, and J. Backman (1989), Pleistocene evolution: Northern Hemisphere ice sheets and North Atlantic Ocean, *Paleoceanography*, *4*, 353–412.

Rühlemann, C., S. Mulitza, P. Müller, G. Wefer, and R. Zahn (1999), Warming of the tropical Atlantic Ocean and slowdown of thermohaline circulation during the last deglaciation, *Nature*, *402*, 511–514.

Rühlemann, C., S. Mulitza, G. Lohmann, A. Paul, M. Prange, and G. Wefer (2004), Intermediate depth warming in the tropical Atlantic related to weakened thermohaline circulation: Combining paleoclimate data and modeling results for the last deglaciation, *Paleoceanography*, *19*, PA1025, doi:10.1029/2003PA000948.

Schmieder, F., T. von Dobeneck, and U. Bleil (2000), The mid-Pleistocene climate transition as documented in the deep South Atlantic: Initiation, interim state and terminal event, *Earth Planet. Sci. Lett.*, *179*, 539–549.

Schneider, R. R., P. J. Müller, and G. Ruhland (1995), Late Quaternary surface circulation in the east equatorial South Atlantic: Evidence from alkenone sea surface temperatures., *Paleoceanography*, *10*, 197–219.

Schneider, R. R., P. J. Müller, G. Ruhland, G. Meinecke, H. Schmidt, and G. Wefer (1996), Late Quaternary surface temperatures and productivity in the east equatorial South Atlantic: Response to changes in trade/monsoon wind forcing and surface water advection, in *The South Atlantic: Present and Past Circulation*, edited by G. Wefer et al., pp. 527–551, Springer, New York.

Schneider, R. R., P. J. Müller, and R. Acheson (1999), Atlantic alkenone sea surface temperature records: Low versus mid latitudes and differences between hemispheres, in *Reconstructing Ocean History—A Window Into the Future*, edited by F. Abrantes and A. C. Mix, pp. 33–56, Springer, New York.

Schulz, M., and K. Statteger (1997), Spectrum: Spectral analysis of unevenly spaced paleoclimatic time series, *Comput. Geosci.*, *23*, 929–945.

Shackleton, N. (2000), The 100,000-year ice-age cycle identified and found to lag temperature, carbon dioxide and orbital eccentricity, *Science*, *289*, 1897–1902.

Shackleton, N. J., and N. O. Opdyke (1976), Oxygen-isotope and paleomagnetic stratigraphy of Pacific core V28–239 late Pliocene to latest Pleistocene, *Geol. Soc. Am.*, *145*, 449–464.

Shackleton, N. J., A. Berger, and W. R. Peltier (1990), An alternative astronomical calibration of the lower Pleistocene timescale based on ODP Site 677, *Trans. R. Soc. Edinburgh Earth Sci.*, *81*, 251–261.

Shannon, L. V. (1985), The Benguela ecosystem, part I: Evolution of the Benguela, physical features and processes, *Annu. Rev. Oceanogr. Mar. Biol.*, *23*, 105–182.

Sinninghe Damsté, J. S., W. I. C. Rijpstra, and G.-J. Reichart (2002), The influence of oxic degradation on the sedimentary biomarker record II: Evidence from Arabian Sea sediments, *Geochim. Cosmochim. Acta*, *66*, 2737–2754.

Stephens, B. B., and R. F. Keeling (2000), The influence of Antarctic sea ice on glacial-interglacial CO_2 variations, *Nature*, *404*, 171–174.

Tziperman, E., and H. Gildor (2003), On the mid-Pleistocene transition to 100-kyr glacial cycles and the asymmetry between glaciation and deglaciation times, *Paleoceanography*, *18*(1), 1001, doi:10.1029/2001PA000627.

van Bennekom, A. J., and G. W. Berger (1984), Hydrography and silica budget of the Angola Basin, *Neth. J. Sea Res.*, *17*, 149–200.

Wefer, G., W. H. Berger, C. Richter, and Shipboard Scientific Party (1998), *Proceedings of the Ocean Drilling Program, Initial Reports*, vol. 175, 577 pp., Ocean Drill. Program, College Station, Tex.

J. H. F. Jansen and J. S. Sinninghe Damsté, Royal Netherlands Institute for Sea Research (NIOZ), P.O. Box 59, 1790 AB Den Burg, Netherlands.

E. Schefuß, Department of Marine Chemistry and Geochemistry, Woods Hole Oceanographic Institution, Woods Hole, MA 02543, USA. (eschefuss@whoi.edu)